Faraday Discussions

Accepted Manuscript

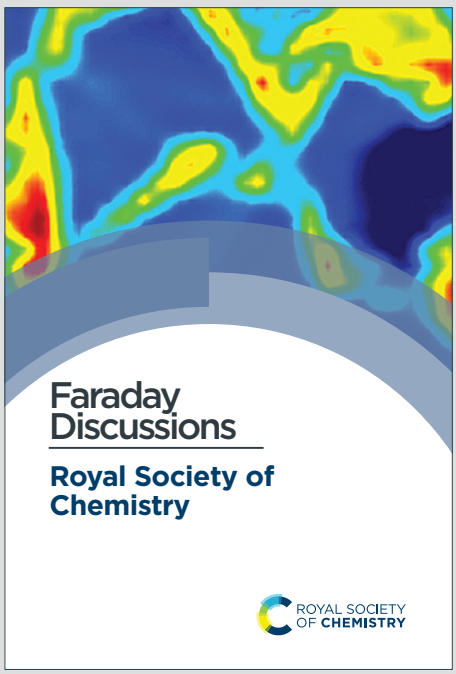

This article can be cited before page numbers have been issued, to do this please use: Y. Chao, A. Marsh, M. Behray, A. Engdahl, F. Guan, Y. Chao, Q. Wang and Y. Bao, *Faraday Discuss.*, 2020, DOI: 10.1039/C9FD00087A.

ROYAL SOCIETY OF CHEMISTRY

www.rsc.org/faraday_d

View Article Online
DOI: 10.1039/C9FD00087A

ARTICLE

Synthesis and Characterisation of Isothiocyanate Functionalised Silicon Nanoparticles and their uptake in cultured colonic cells

Received 00th January 20xx,
Accepted 00th January 20xx

DOI: 10.1039/x0xx00000x

Yimin Chao[a†], Ashley I. Marsh[a], Mehrnaz Behray[a], Feng Guan[ab], Anders Engdahl[c], Yueyang Chao[d], Qi Wang[e], and Yongping Bao[e]

The functionalisation of silicon nanoparticles with a terminal thiocyanate group, producing isothiocyanate-capped silicon nanoparticles (ITC-capped SiNPs) has been successfully attained. The procedure for synthesis is a two-step process that occurs via thermally induced hydrosilylation of hydrogen terminated silicon nanoparticle (H-SiNPs) and further reaction with potassium thiocyanate (KSCN). The synthesis was confirmed by Fourier Transform Infrared (FTIR) spectroscopy and X-Ray Photoelectron Spectroscopy (XPS). At the same time, the internalisation and the cytotoxicity of ITC-capped SiNPs in vitro was assessed in two cell lines: Caco-2, human colorectal cancer cells and CCD-841, human colon "normal" cells. The results showed that above concentrations of 15 μg/ml, the cell viability of both cell lines depleted significantly when treated with ITC SiNPs, particularly over a 48 hour period, to approximately 20% cell viability at the highest treatment concentration (70 μg/ml). Flow cytometry was employed to determine cellular uptake, in Caco-2 cells treated with ITC SiNPs and it was observed that at lower SiNP concentration, uptake efficiency was significantly improved at a time period under 12 hours; overall it was noted that cellular uptake was positively dependent on the period of incubation and the temperature of incubation. As such, it was concluded that the mechanism of uptake of ITC SiNP was through endocytosis. Synchrotron FTIR spectroscopy, by means of line spectral analysis and IR imaging, provided further evidence to suggest the internalisation of ITC SiNPs displays a strong localisation, with an affinity for the nucleus of treated Caco-2 cells.

1. Introduction

In the US alone it is predicted that there will be a total of 1,735,350 new cases of cancer diagnosed and up to 609,640 fatalities owing to cancer in the year of 2018.[1] Both figures were higher than in 2017, with an increase of 46,570 and 8,720 respectively. Whilst survival rates of cancer are projected to double by 2030 in the UK, the number of cases in the UK alone has risen by 500,000 in the years of 2010~2015 and is projected to increase from 2.5 million to 4 million by 2040.[2] Despite the increase in survival rate however, some of the principles behind some the most successful and frequently employed anti-cancer treatments are proving to be almost as harmful to patients as cancer itself. Traditional anti-cancer treatments and therapies, such as chemotherapy and radiotherapy, despite their success can lead to the onset of a number of physical and psychological side effects such as long term cardiovascular disease, cognitive and neurological deficits and bone density reductions.[3-5]

Consequently, a lot of time and money is being invested on the development of nanoscale therapeutic agents that can be employed to provide a safer, time efficient, more direct route to identification, diagnosis and treatment of cancer as well as a whole host of other diseases. The functionalisation of silicon quantum dots with ligands that exhibit anti-cancerous properties holds several advantages versus traditional therapy. One functional group that has been extensively proven to inhibit carcinogens is isothiocyanates (ITC).[6, 7]

ITC have been identified as a highly effective chemopreventitive group of molecules that are associated with a number of anti-cancerous processes, namely the prevention of propagation of carcinogen activating phase I enzymes, the induction of arrests in cell cycles, leading to apoptosis of genetically mutated cells, and the induction of phase II enzymes that act as carcinogen detoxifiers.[8, 9]

Phase II enzymes such as quinone reductase (QR) and glutathione S-transferase (GST) have been identified as potent detoxifying enzymes that can reduce the onset of chemical carcinogenesis, in effect preventing the initiation of malignant and invasive cell behaviour.[10] It has been well documented that a number of naturally occurring isothiocyanates, found in cruciferous vegetables, are able to not only prevent the initiation of carcinogenesis but further inhibit the progression of tumorigenesis by increasing the tissue levels of these detoxifying enzymes in a number of rat tissues.[8, 11]

[a] School of Chemistry, University of East Anglia, Norwich NR4 7TJ, United Kingdom.
[b] MAX IV laboratory, Lund University, P. O. Box 118, 22100 Lund, Sweden.
[c] School of Pharmacy, Heilongjiang University of Chinese Medicine, Haerbin 150040, China.
[d] Birmingham Heartlands Hospital, Bordesley Green E, Birmingham B9 5SS, United Kingdom.
[e] Norwich Medical School, University of East Anglia, Norwich NR4 7TJ, United Kingdom.
† corresponding author. Y.chao@uea.ac.uk
Electronic Supplementary Information (ESI) available: [details of any supplementary information available should be included here]. See DOI: 10.1039/x0xx00000x

This type of interaction does not rely on the binding of ITCs to specific enzymes and thus occurs as an indirect interaction, however the ability for ITC compounds to perform such a role has a reliance on direct interactions and binding mechanisms to well identified targets. A number of studies have focused on the effects of plant derived isothiocyanates and the effect on carconogesis.[12, 13] Herein, we present an investigation utilising silicon nanoparticles (SiNPs) functionalised to contain a terminal isothiocyanate group in order to more fully develop and utilize it.

The use of silicon nanoparticles as observable carriers for chemopreventitive molecules holds a number of advantages over traditional fluorophore and/or heavy metal nanoparticle systems. Silicon nanoparticles offer a material with a broad excitation spectrum, which is tuneable by size, owing to the quantum confinement effect.[14] Traditional dyes such as fluorescein or rhodamine cannot provide such favourable characteristics in comparison. Therefore, from a biomedical standpoint, the main advantage of this effect is their use in multi-coloured quantum dot probes. The inherent photoinduced bleaching effects observed with traditional dye methods can be overcome by utilising silicon nanoparticles that provide a much more photostable alternative for 3D imaging.[15] Photoinduced cytotoxicity is an issue that has been reported when utilising traditional dyes and has resulted in the formation of free radicals and singlet oxygen.[16]

Moreover, group II-VI heavy metal core nanoparticles provide size tuneable optical properties and a high quantum yield much in the same way that silicon quantum dots are able to.[17] However upon exposure to aqueous environments or irradiation by UV light, Cadmium based quantum dots have demonstrated core material leakage, leading to preventative measures being put in place to inhibit cytotoxicity.[18-20]

In this investigation, hydrogen terminated SiNPs (H-SiNPs) were prepared by the electrochemical etching of porous silicon. These H-SiNPs were reacted with allyl bromide in a hydrosilylation reaction and the resulting bromine terminated nanoparticles (Br-SiNPs) refluxed with potassium thiocyanate to produce ITC terminated silicon nanoparticles (ITC-SiNPs). And the resultant ITC-SiNPs were examined in terms of their cytotoxicity, cellular uptake efficiency and cellular internalisation in colorectal cancer cells and primary cells.

2.1 Chemical Properties

As confirmation that the silicon nanoparticle surface was successfully functionalized with the isothiocyanate ligand, FTIR measurements in transmission mode were taken. The obtained spectra (Figure 1) were measured using nanoparticle samples dissolved in distilled toluene.

The peak visible at about 2080 cm^{-1} is a clear indicator of the presence of Si-H band. The observed features at 1259 cm^{-1} at 1454 cm^{-1} can be ascribed the symmetric bending modes and vibrational scissoring modes of Si-CH_2 respectively, whilst the dominant feature at 1020 cm^{-1} is indicative modes of silicon surface oxidation and characteristic of Si-O bonds.[21, 22] The polarity of this bond in particular is what extenuates it's observed transmittance.[23] All major data are listed in Table 1.

The surface properties of the functionalized nanoparticles were investigated utilising X-Ray Photoelectron Spectroscopy. The full survey spectra of ITC SiNPs can be found in Figure 2a, whilst high resolution spectra representing the N1s, C1s and Si2p orbitals are displayed in Figure 2b-d. Spectrum displayed in

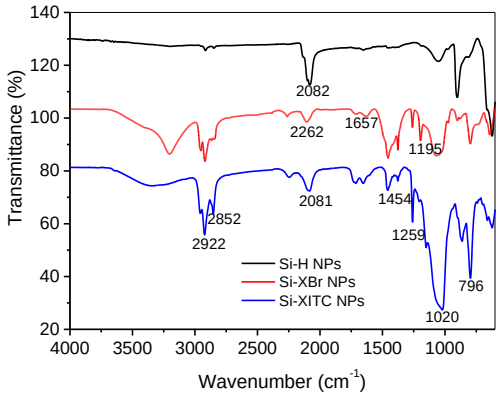

Figure 1 FTIR spectra of H-terminated SiNPs, Allyl bromide capped SiNPs, and ITC-capped SiNPs.

2. Results and discussion

Table 1 FTIR spectra Features of ITC and Allyl bromide functionalised $SiNP_S$.

SiNPs	Si-C	Si-O	C = S	-CH_2	-CH_2-	C=N	Si-H	=C=N-	-CH_2-	-CH_2-
ITC-capped		1020	1195	1259	1454	1657	~2080	2262	2852	2922
Allyl bromide capped	~800	1020	1195	1259	1454	1657	~2080	2262	2852	2922
H-terminated	~800	1020					~2080			

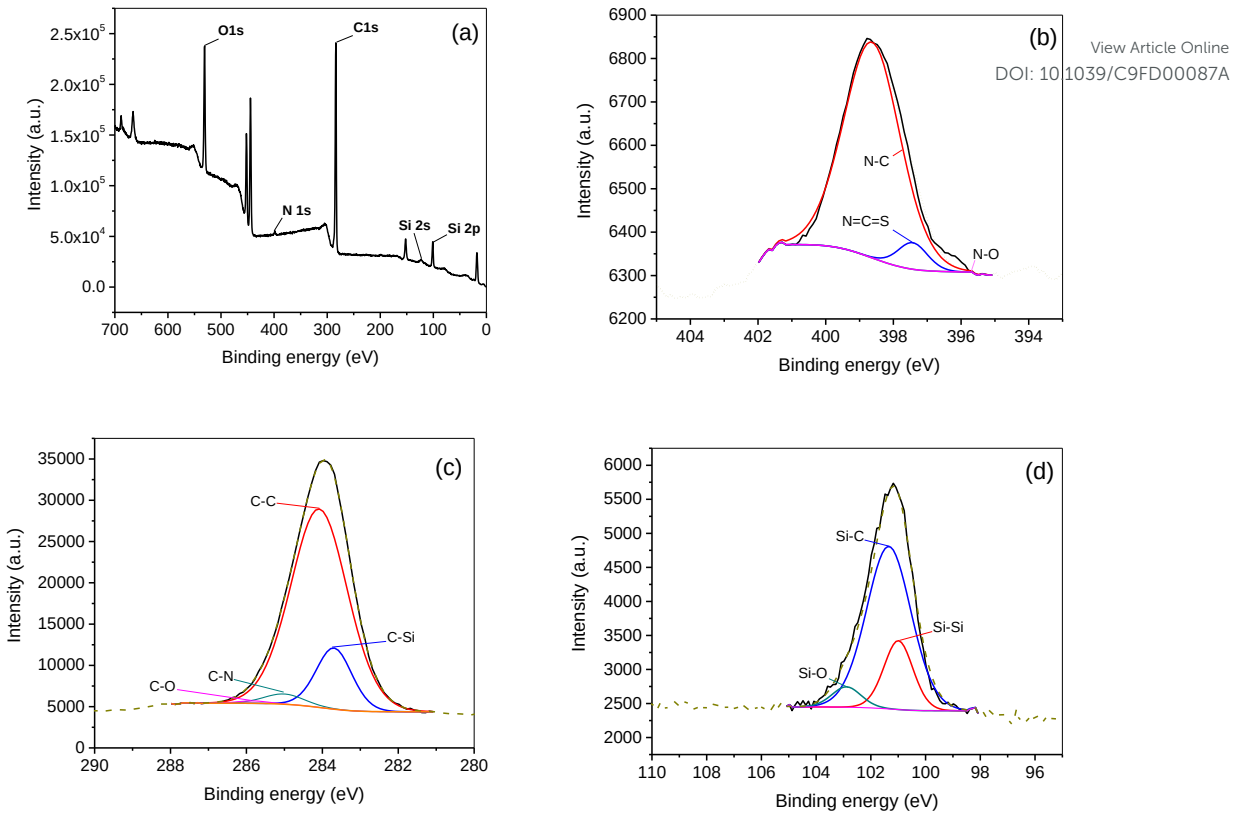

Figure 2 XPS Spectra obtained from ITC-functionalised SiNPs (a) ITC Full survey spectrum, (b) N 1s, (c) C 1s, (d) Si 2p. Dotted lines correspond to the fitting obtained by the spectrum components.

Figure 2b corresponds to the high resolution N 1s spectrum. It was fitted with three components and a Shirley Background. The three observed peaks correspond to N=C=S at 397.5 eV, N-C at 398.7 eV and N-O at 399.3 eV. The C1s peak observed in Figure 2c was subjected to four components being fitted and a Shirley background. The four peaks observed correspond to C-Si, C-C, C-N and C-O bonding at 283.7, 284.1, 285.0 and 285.4 eV respectively. Figure 2d shows the high resolution spectrum of Si 2p, which was fitted with three components and a Shirley background. The three observed peaks appear at 102.8, 101.4 and 100.8 eV. The first peak is believed to arise from Si-O bonding. The peak at 101.4 eV is representative of Si-C bonding and the third peak at 100.8 is taken to be characteristic of Si-Si bonding. According to the surface chemistry data obtained from XPS, the surface of SiNPs is fully capped with the thiocyanate group. The presence of ITC functionality has also been confirmed by Energy-dispersive X-ray spectroscopy (EDX) mapping of the particles (Figure S1). The disappearance of Br signal in ICT-SiNP EDX suggested that all the surface Br moieties have been converted to ITC groups (Figure S1).

2.2 Optical Properties

Figure 3a displays the emission and absorption spectra of ITC SiNPs in distilled toluene, measured at room temperature. The solid line represents the photoluminescence emission spectrum of the ITC SiNPs that were subject to an excitation wavelength of 360 nm. The maximum observed emission was centred at approximately 430 nm, characteristic of blue light emission In the UV-vis spectra (Figure 3) obtained there was a clear increase in the absorbance detected when decreasing the excitation wavelength from approximately 500 nm, a characteristic feature of the absorption corresponding to the indirect bandgap semiconductors such as silicon.

The fluorescence quantum yield was measured and calculated according to the method outlaid by Williams et al, with 0.1M H_2SO_4 as the reference for measurements.[24] As detailed in supporting information Figure S2 and S3, it was observed that for ITC SiNPs, at an excitation wavelength of 360 nm, the photoluminescence quantum yield (PLQY) was measured to be about 13%, which complies with previous investigations that cite values of up to 25% PLQY.[25-27]

2.3 Particle Size

To determine the mean size and polydispersity of ITC-capped silicon nanoparticles, TEM images and XRD and DLS spectra were obtained. Figure 4 displays the obtained TEM spectra of a sample of ITC SiNPs data that displays the range of sizes obtained from these images. From 100 random nanoparticles it was observed that the sample ITC SiNPs had a mean diameter of 4.01 nm. The observed polydispersity in these values can be attributed to the lattice spacing of silicon crystals. Results obtained by DLS and the value for the mean diameter calculated utilising XRD, concurs with this value and these results can be found in the supplementary information (Figure S4 and S5).

Deviations in the values of diameter calculated are likely due to the differing individual methods used for size calculation. It is

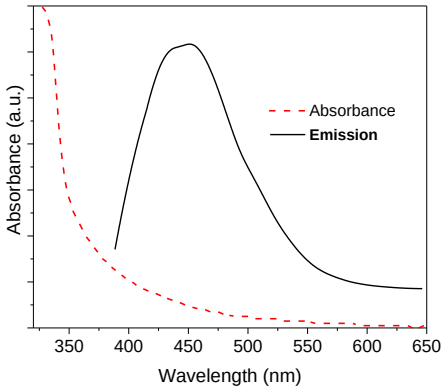

Figure 3 Absorption and emission spectra of ITC SiNPs with excitation wavelength of 360 nm.

highly likely that due to the low electron density of the ITC chain that only the silicon core of our ITC SiNPs is measurable by TEM. Meanwhile values obtained by DLS can be taken only as an estimate of the hydrodynamic radius, that is the hypothetical size value of a solid sphere that diffuses in the same manner as our nanoparticles, as calculated by the Stokes-Einstein relation. Values obtained by utilising XRD spectra and the Scherrer equation can similarly be regarded as no more than an estimate.

2.4 Cellular Internalisation

2.4.1 Internalisation of ITC SiNPs observed by Confocal Microspectroscopy

In this experiment, Caco-2 colonic cancer cells were treated with a solution of ITC SiNPs with a concentration of 50 µg/mL. Cells were incubated with the ITC SiNPs for 6 and 12 hours at a temperature of 37 ºC. The series of images detailed in Figure 5 a show the fluorescence exhibited under confocal microscopy due to 1) Phalloidin, used to stain actin, in red 2) ITC SiNPs which in this case is null due to these being images of control cells, in green and 3) a combined image of both phalloidin and ITC SiNP fluorescence. In Figure 5b2 the cellular internalisation of ITC SiNPs after 6 hours incubation is displayed. What was noted when comparing Figure 5b2 and 5c2 is that the internalization and localization of ITC SiNPs was clearly time dependent, given that the image obtained after 12 hours, Figure 5c3, exhibits much more intense ITC SiNP fluorescence and clearly a higher number of ITC SiNPs were observed.

2.4.2 Internalisation of ITC SiNPs observed by Synchrotron FTIR

Both Caco-2 and CCD cell lines were treated with a 50 µg/ml ITC SiNPs' solution for 6 hours prior to point spectroscopy measurements being taken. Each measurement consisted of a minimum of 8 points selected across the cell for IR identification, along with this a visual image and protein specific IR image was taken by using the integrated absorbance of the amide I region between 1600~1700 cm^{-1}, a critical band which arises due to the stretching of C=O contained in the peptide bonds of the proteins within the cell. This gives an indication of protein distribution when treated as shown in Figure 6a and Figure S6, and untreated, Figure 6b and Figure S7.

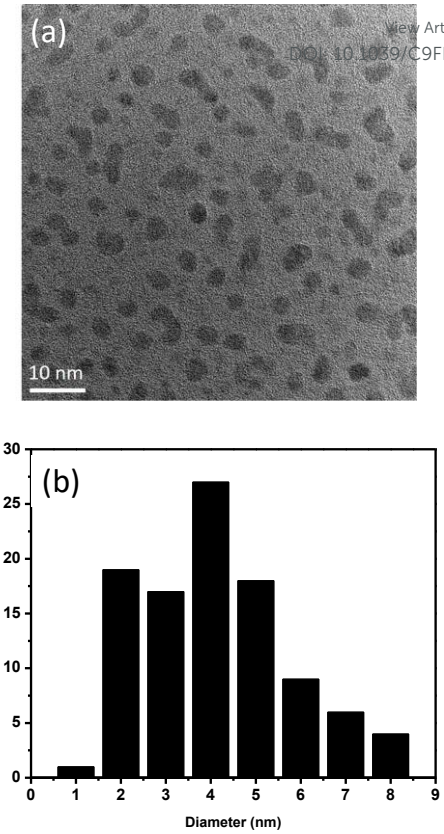

Figure 4 TEM images of ITC-functionalized SiNPs drop cast onto a copper grid with inset values of a) 2 nm b) 5 nm c) 10 nm and d) 20nm and e) corresponding histogram of sizes obtained.

Comparing the IR images obtained for the treated and untreated Caco-2 cells, the first striking difference was the relative uniformity of protein concentration throughout large parts of the untreated cell compared to what appears to be nucleus localisation in those treated with ITC SiNPs. The line spectra confirm the observations taken from the IR images, as can be seen when highlighting the aforementioned amide I region between 1600~1700 cm^{-1}. It was noted that the intensity of the peak in this region remained the same throughout the untreated cell, whereas it was clear that converging upon the nucleus in the untreated Caco-2 cell, that the peak intensity increased, with the topmost absorbance observed within the

View Article Online
DOI: 10.1039/C9FD00087A

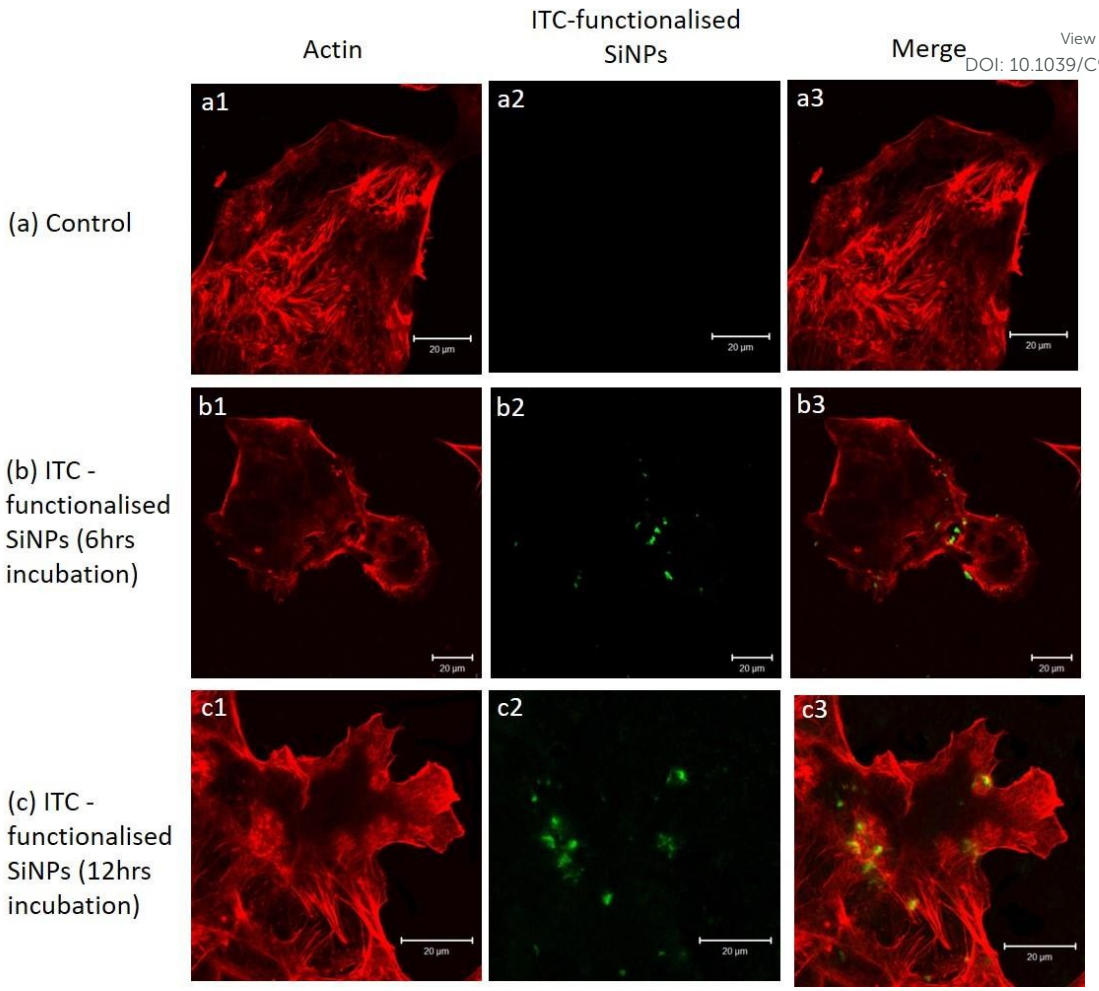

Figure 5 Confocal fluorescence images of Caco-2 cells a) treated with no ITC-functionalised SiNPS (control) and Caco-2 cells incubat-ed with ITC -functionalised SiNPs for b) 6 hours and c) 12 hours. Red fluorescence corresponds to Phalloidin staining of Actin and green corresponds to ITC-functionalized SiNPs.

nucleus. A number of features that correspond to the vibrations of DNA and phospholipid can be observed when comparing treated and untreated cells. At the nucleus in particular it was seen that the vibration around 1078 cm^{-1}, corresponding to phosphodiester groups in DNA, changed in both cell lines, indicating changes in the DNA environment and a shift in DNA distribution across the cell.

Differences in the phospholipid content within the cellular membrane has given rise to a new peak at 1737 cm^{-1} which corresponds to C=O stretching, and an increase in the C-H absorption observed between 2800~3050 cm^{-1}. These features indicate an increase in the phospholipid content in this area of the cell. Changes in the cell membrane content have been described previously in work using a number of inducing molecules, including ITC, citing apoptosis as a consequence of these cellular alterations. [28, 29] Further literature concurs that isothiocyanate has been proven to induce apoptosis.[30, 31]

The observed concentration of proteins in the nucleus after treatment with ITC concurs with several publications which note the translocation of Nrf2 to the nucleus following transfection with extracellular kinases which occurred as a result of the chemical stress caused by the introduction of ITC. [7, 32, 33]

A similar outcome was observed when comparing the IR spectra obtained treated and untreated CCD-841 cells, in Figure 6c-d. The same fluctuation in absorbance in the amide I band was observed moving from the space outside the cell, through the cytoplasm and nucleus.

2.5 Cell Viability by MTT Assay

In order to obtain a measure for the cell viability and cytotoxicity of cells treated with ITC functionalised SiNPs, an MTT assay was performed on both Caco-2 and CCD-841 cell lines, treated with ITC SiNPs. As a control, amine capped SiNPs, that have been established as a non-cytotoxic, monitor able biological substance. [34] The assay was replicated over time periods of 24 and 48 hours to investigate the potential longer term effects of treatment citing ITC SiNPs, as indicated in Figure 7.

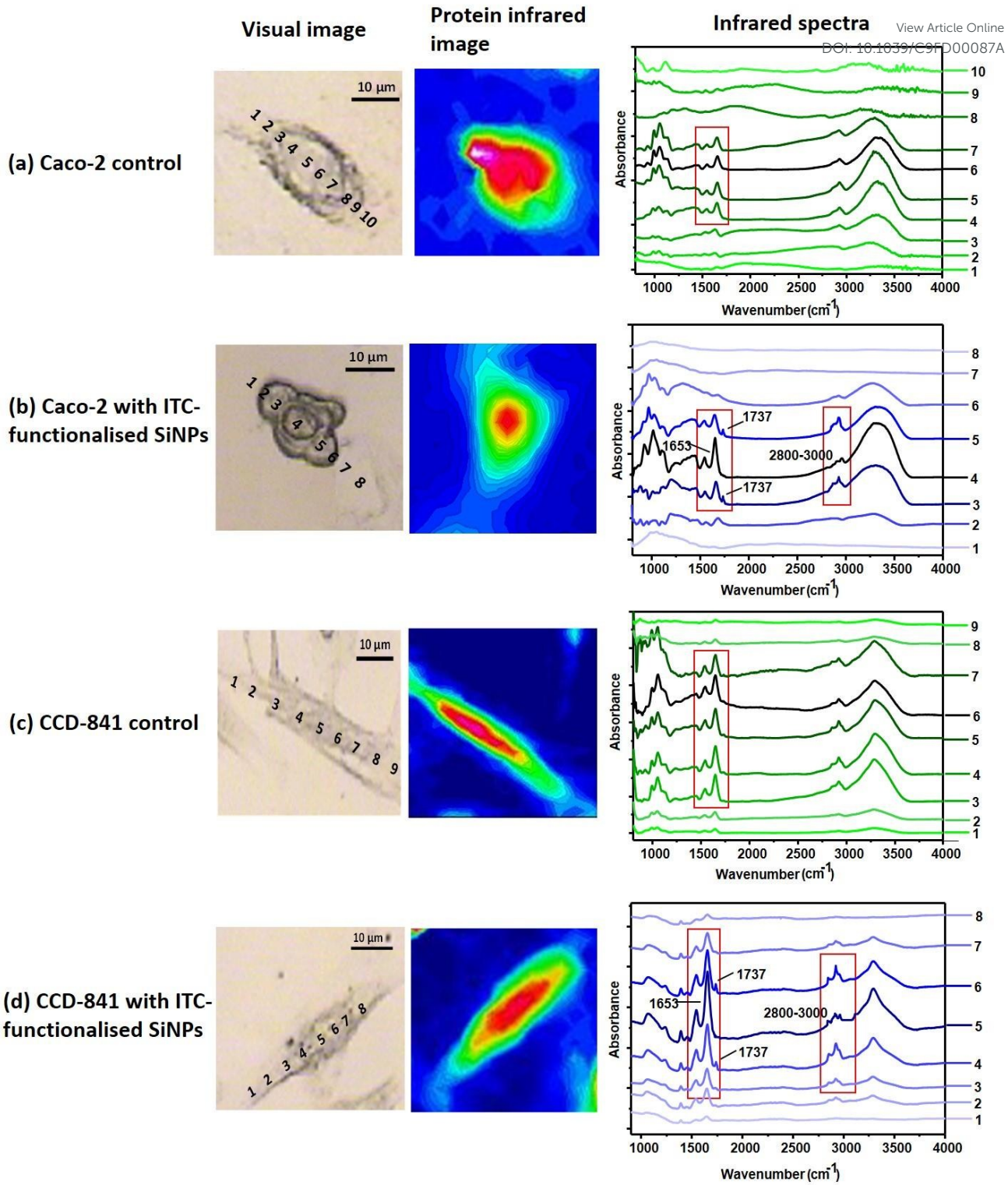

Figure 6 Visual image, protein infrared image and corresponding infrared spectra acquired along the line of a Caco-2 control cell (a), a Caco-2 cell treated with ITC-functionalised SiNPs (b), a CCD-841 control cell (c), a CCD-841 cell treated with ITC-functionalised SiNPs (d).

After an incubation period of 24 hours, at concentrations of 15 μg/ml and below for both cell lines, it was observed that both nanoparticle systems performed with relative parity with regards to the viability of the cells treated. From herein, at concentrations above 15 μg/ml, it was noted that the cell viability of both lines when treated with ITC SiNPs suffered an immediate reduction of approximately 20%, in stark contrast to the control cells which from this point, maintained relatively

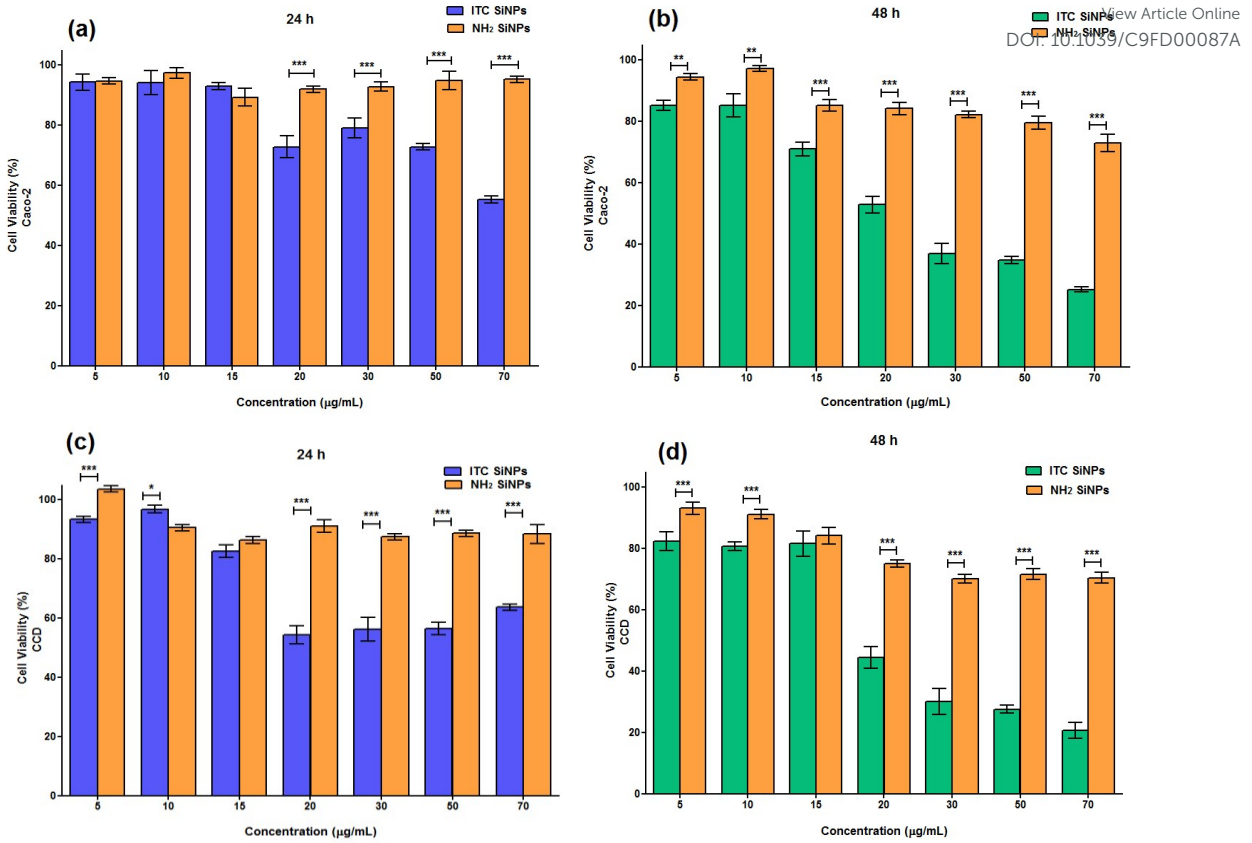

Figure 7 Cell viability results of Caco-2 cells treated with ITC SiNPs after a) 24 hours incubation and b) 48 hours incubation time, and CCD-841 cells treated with ITC-functionalised SiNPs after c) 24 hours incubation and d) 48 hours incubation, with NH_2-functionalised SiNPs as a control. Statistical significance was determined by two-way-ANOVA followed by a Bonferroni post-test. (***P < 0.001, **P < 0.01, *P < 0.05). Results are expressed as mean ± SEM (n =3).

stable viability values of 90% and 80% in Caco-2 and CCD-841 lines respectively.

The viability data obtained after 48 hours incubation in both cell lines showed a much more dramatic and clearer reductive trend in cell viability with increasing ITC SiNPs' concentration. This effect again becomes particularly apparent at concentrations above 15 µg/ml. Below 15 µg/ml however there was no observed statistical difference in the cell viability of ITC treated CCD-841 cells after 48 hours, the same is said for Caco-2 cells treated with ITC at low concentrations of 5 and 10 µg/ml.

The cytotoxic nature of ITC SiNPs is highlighted in the steady reduction of cell viability from 80% at 10µg/ml to just above 20% at the highest concentration; it's effect on healthy CCD cells however was more dramatic, resulting in the immediate loss of approximately 40% viability at 20µg/ml and a steady decline from 40% to 20% cell viability thereafter up to the maximum concentration.

As expected, after 48 hours incubation, control cells treated with amine capped SiNPs produced similar results in both healthy and unhealthy cell lines, and overall displayed a significantly reduction in the cell viability from lower to higher concentrations, resulting at its lowermost, cell viability of 70%~80% in both lines.

By varying both time and concentration of cells incubated with ITC SiNPs, this study provided further evidence for the relatively low cytotoxicity of amine capped silicon nanoparticles and a large time and concentration dependence on the reduction of cell death in healthy and cancerous cell lines treated with ITC SiNPs. Whilst this is the desired effect for cancerous cells treated with this ITC system, it is worth noting that particularly with increased incubation; the observed cytotoxicity in healthy CCD cells provides no more benefit than traditional the already well-established chemopreventitive treatments.

2.6 Cellular Uptake and Uptake Efficiency

The efficiency of cellular uptake, which takes into account the fluorescence of cells treated with ITC SiNPs relative to unstained control cells, was measured at both concentrations at four incubation periods between 6 and 48 hours as detailed in Figure 8a.

The relative fluorescence of cells treated with 20 µg/ml ITC SiNPs steadily raised from 8 to 20% as incubation increased, contrasting largely to those treated with the higher concentration (70 µg/ml) of ITC SiNPs. The median fluorescence observed remained virtually unchanged between 6 and 12 hours of incubation, meaning at 12 hours that at both concentrations of SiNP, the observed fluorescence was close to

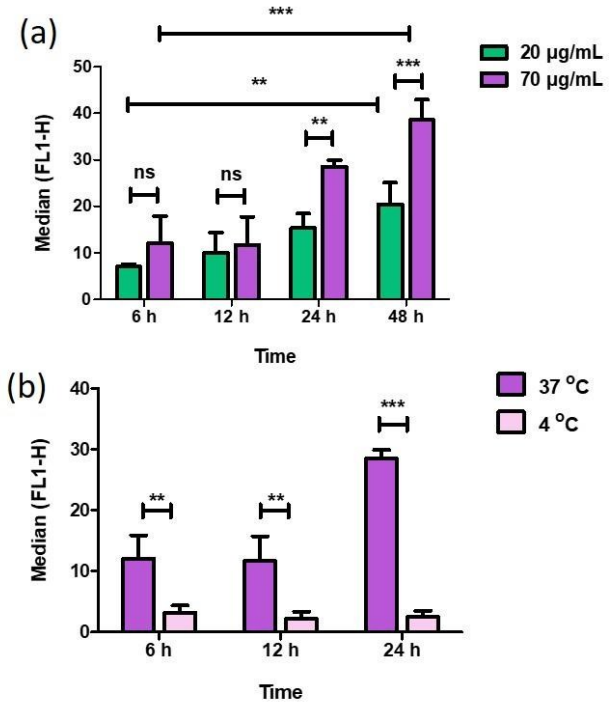

Figure 8 Flow cytometry results, displaying a) cellular uptake as the fluorescence median of cells treated with ITC-functionalized SiNPs vs. time at SiNP concentrations of 20 and 70 µg/ml. b) cellular uptake as the fluorescence median of cells treated with ITC-functionalized SiNPs vs. time at incubation temperatures of 37 °C and 4 °C

parity. At this point it can be said that the uptake efficiency of cell treated with the lower concentration of SiNPs was higher than that of those treated at a higher dose.

Above 24 hours of incubation however, cells treated with 70 µg/ml displayed a far superior fluorescence by comparison to those treated at a lower concentration.

As it was the case that the median fluorescence observed was higher in those cells treated with a higher concentration of ITC SiNPs, and given that the general trend observed with increasing incubation time was one of increased fluorescence, it can be stated with confidence that the cellular uptake of ITC SiNPs displays a dependence on both time and concentration. However, to gain more of an understanding of the mechanism of ITC uptake within the treated cells, it was important to identify whether their cellular uptake exhibited a relationship with the temperature of incubation. It is well documented that along with sample viscosity and material size, that the rate and uniformity at which molecules are transported and diffused across the cell membrane is highly dependent on temperature.[23]

Endocytosis is generally accepted as being the most populous mechanism amongst nanoparticles at sizes above 5 nm, and uptake efficiency by this mechanism has been largely linked to the physical and chemical parameters of the materials uptaken.[35]

Caco-2 cells were treated with the highest concentration (70µg/ml) of ITC SiNPs and incubated over three periods of time between 6 and 24 hours, at 4 and 37°C, as detailed in Figure 8b. It was found that cellular uptake, particularly in the period of 12 to 24 hours, displayed a vast increase at 37 °C whilst at the lower temperature, this value remained virtually unchanged overtime. What this indicated is that the mechanism dictating Caco-2 cell membrane penetration by ITC SiNPs depends as much on environmental factors as nanoparticle concentration.

3. Experimental Methods

3.1 Synthesis Procedure of ITC-capped SiNPs

A layer of porous silicon with terminal hydrogen was synthesized by the galvanostatic anodisation of boron-doped porous silicon p-Si (100) chip, 1.3×1.3 cm, 1~10 Ωcm^{-1} resistivity(PI-KEM Ltd, Tamworth, UK) in a 1:1 (v/v) solution of ethanol and 48% aq. HF, in a modification to the method established by Chao et al.[36] The resulting hydrogen terminated SiNPs were reacted with allyl bromide (2 ml) under reflux for 18 hours in distilled toluene. The result was a yellow-orange solution which when irradiated by UV light exhibited an orange-red visible photoluminescence. The solution was dried under reduced pressure at 60 °C resulting in approximately 30 mg allyl bromide terminated SiNPs.The resulting nanoparticles were redispersed in distilled EtOH (10 ml), and potassium isothiocyanate (KSCN) was added in a 0.6:1 ratio of KSCN : allyl bromide terminated SiNPs and the mixture left to reflux for 18 hours. The solution was allowed to cool before being dried under reduced pressure. The product obtained was dissolved in 3×10 ml diethyl ether and washed with 3 ×12 ml deionised water. The yellow, translucent organic layer was dried and filtered, and the solvent was removed from filtrate by drying under vacuum, resulting in an average of 10 mg ITC-capped SiNPs. The process principles of the above two steps are explained in Scheme 1.

3.2 Chemical Properties Analysis

FTIR measurements were carried out using a PerkinElmer ATR-FTIR spectrometer and conducted on solid hydrogen, allyl bromide and isothiocyanate terminated silicon nanoparticle samples. Spectra were obtained after 16 scans following background correction.

View Article Online
DOI: 10.1039/C9FD00087A

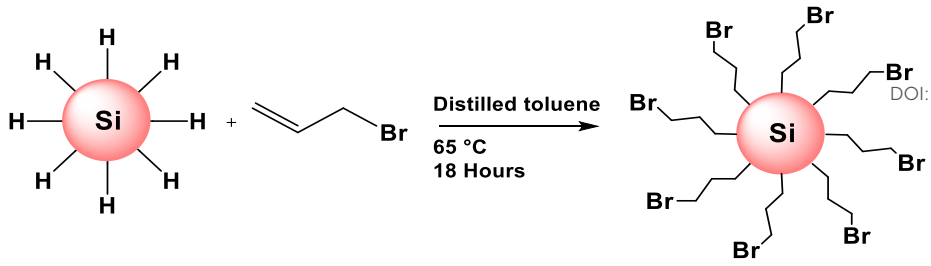

a)

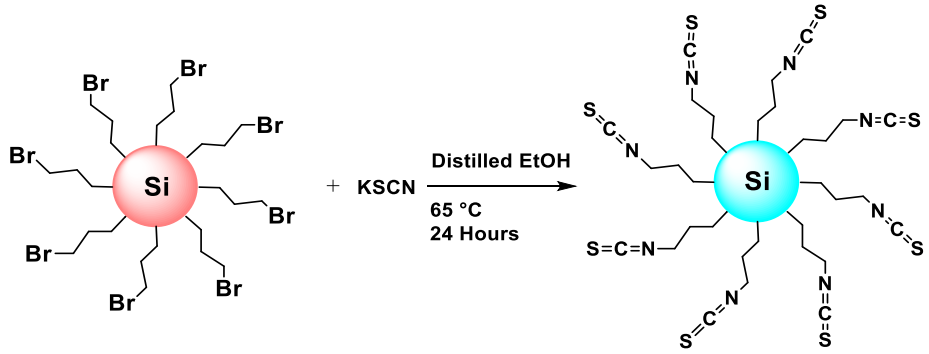

b)

Scheme 1 Schematic representation of the two-step synthesis of ITC SiNPs. a) The thermally induced hydrosilylation of hydrogen terminated SiNPs with allyl bromide, b) The subsequent reaction between allyl bromide functiojnalised SiNPs and KSCN.

XPS measurements were conducted using a K-Alpha XPS Instrument at NEXUS, Newcastle, UK. The solid sample was pressed into 1×1 cm indium foil substrate (0.5 mm thickness, 99.999% trace metals basis, Sigma-Aldrich). The foil was placed in a N_2 load-lock for drying before being placed under ultra-high vacuum conditions, with pressure under $5x10^{-9}$ mbar. All obtained spectra were acquired at room temperature and normal emission using Al Kα radiation. All values of binding energy (BE) were referred to the $In3d_{5/2}$ peak obtained from the measurement of Indium foil in direct contact with the ITC SiNPs, which was observed at a BE of 444 eV.

3.3 Optical Properties

All optical measurements were conducted on samples of ITC SiNPs dispersed in distilled toluene. Quinine hemisulphate salt monohydrate diluted in 0.1 M H_2SO_4 was used to obtain reference UV-vis and PL spectra.

UV-vis absorption (UV-vis) spectra of ITC–terminated SiNPs were obtained on a PerkinElmer 35 UV-vis double beam spectrometer in a quartz cuvette (10 mm ×10 mm). The scan range was 200~800 nm with a scan speed of 200 nm/min. Prior to each measurement, a baseline scan of distilled toluene was performed to be subtracted from the subsequent sample spectra. Photoluminescence emission (PL) spectra were recorded on the PerkinElmer LS55 spectrometer in a quartz cuvette (10 mm × 10 mm). The spectrometer scan range was set to 370~800 nm, with a fixed excitation of 360 nm, excitation slit width of 12.5 nm and emission slit of 2.5 nm. All emission spectra were corrected using the solvent spectrum as the background.

The photoluminescence quantum yield (QY) of ITC SiNPs was obtained using Quinine Sulphate, with a known QY of 54.6% in 0.5 M H_2SO_4, as a standard. The absorbance and emission spectra obtained for ITC SiNPs and quinine sulphate shows the gradient of the plotted integrated intensity of ITC SiNP (in distilled toluene) and quinine sulphate (in 0.1M H_2SO_4) solutions with recorded absorbances of between 0.1 and 0.01. Utilising the calculated gradients of these plots and the known quantities of solvent refractive indices and QY of quinine sulphate, a value of photoluminescence quantum yield for these ITC SiNPs could be generated using the following equation:

$$Q = Q_R \left(\frac{grad_S}{grad_R}\right)\left(\frac{\eta^2}{\eta_R^2}\right)$$

where Q is the quantum yield, grad refers to the gradient obtained from a plot of integrated fluorescence emission intensity vs. absorbance for the sample, and η is symbolic of the refractive index. The subscript's S and R express the sample and reference respectively.

3.4 Particle Size Measurements

Dynamic Light Scattering (DLS) was used to measure the hydrodynamic radius and polydispersity index of ITC-capped SiNPs dispersed in distilled toluene. Spectra were obtained with a Zetasizer Nano ZS (Malvern Instruments Ltd, Worcestershire, UK) and a triplet of measurements taken for each sample solution. Measurements were taken at 20 °C with a 30 second equilibration preceding each set of measurements.

X-Ray Powder Diffraction (XRD) measurements were undertaken utilising the ARL XTRA Powder Diffractometer (Thermo Scientific, USA) in order to obtain the crystallinity and the mean nanoparticle size of ITC SiNPs. Applying Scherrer's equation to the obtained spectra it is possible to calculate an estimate for the mean size of a powder sample τ:

$$\tau = \frac{k\lambda}{dcos\theta}$$

where k is a shape factor, typically taken as 0.9, λ is the wavelength of the incident X-ray, d is the full width half maximum (FWHM) of the peak in radians, also denoted as Δ(2θ) and θ is the Bragg angle in degrees.

Transmission electron microscopy (TEM) studies were performed on the JEOL, JEM 2100 microscope running a LaB_6 (lanthanum hexaboride crystal) emitter and an applied voltage of 200 kV. TEM samples were prepared by drop-casting a dilute suspension of the sample dispersed in distilled ethanol onto a 200-mesh carbon-coated copper grid. The grids were dried before the measurement. TEM micrographs were taken at different spots of the grid.

3.5 Cell Culture

Two cell lines, Caco-2 and CCD-841, corresponding to human colorectal adenocarcinoma and human normal colon epithelial cells respectively, were sub-cultured in RPMI appended with 10% fetal bovine serum, 2 mM L-glutamine, 100 µg/mL streptomycin and 100 µg/mL penicillin. Incubation and maintenance occurred at a temperature of 37 °C under a 5% CO_2 atmosphere. Both cell lines exhibited negative results for mycoplasmosis.

3.6 Cellular Internalisation

Initially, Caco-2 cells were seeded in a 12-well plate, covered by glass slips. After 24 hours, the cells were incubated for 6 and 12 horus respectively with 50 µg/mL ITC SiNPs. Following this incubation period, cells were washed and fixed with 4% (v/v) paraformaldehyde (Sigma-Aldrich) in phosphate buffered solution (PBS), at room temperature for 20 minutes.

Actin present within the cells was stained using 6.6 µM Texas Red-X Phalloidin (Life Technologies). Laser Scanning Confocal Microscopy (LSCM) was conducted on a Zeiss LSM510 META confocal microscope, utilising a 63× oil immersion objective lens. The excitation wavelengths of the beams exciting the ITC SiNPs and actin were 488 nm and 543 nm respectively.

3.7 Cytotoxicity

Both cell lines were subjected to standard MTT assays to determine the cytotoxicity of ITC SiNPs. Each line was seeded into a 96 well plate at a density of 4.5×10^{-5} cells per well and left for 24 hours. After this, the media used in seeding was removed and replaced with varying concentrations of ITC SiNP solution. The ITC SiNP suspension were concentrated with values of 5, 10, 15, 20, 30 50 and 70 µg/mL. Each concentration and time grouping were replicated a minimum of three times and results normalised against untreated control. The absorbance of the resultant wells was measured using the BMG Labtech Polar Star Optima at a wavelength of 570 nm with results expressed as mean values ± standard deviation.

3.8 Flow Cytometry

Both cell lines were seeded in 24 well plates at a seeding density of 5×10^4 cells per well. Both were treated with ITC SiNPs at concentrations of 20 and 70 µg/mL for time periods of 6, 12, 24 and 48 hours. Following trpsyinisation, the cells were washed three times with PBS and centrifuged for 5 minutes at 1200 rpm between washes. Cells were fixed with 4% (v/v) paraformaldehyde in fetal bovine serum for 20 minutes and washed with PBS. Cells were re-suspended in a buffer of 5 % (v/v) fetal bovine serum in PBS prior to flow cytometry measurements. 10,000 gated cells were examined for cellular uptake by observing ITC SiNP fluorescence using the FL1 channel detector and a BD FACSCalibur (BD Bioscience). Each ceoncentration and time pairing was performed three times on different SiNP samples. Data was analyzed with CellQuest Pro® software (BD Biosciences) and values presented as median ± standard deviation.

View Article Online
DOI: 10.1039/C9FD00087A

3.9 Synchrotron FTIR

High Resolution Synchrotron FTIR microscopy was performed at the Max IV Laboratory facility and measurements were taken using the Bruker IFS66V FTIR spectrometer linked to a Hyperion 3000 IR microscope utilising synchrotron radiation as the illumination source. Operating in transmission mode with a 10×10 μm^2 aperture, 15× objective lens, a single condenser and a 100×100 μm^2 Mercury Cadmium Telluride (MCT) detector, the video linked microscope achieved a magnification of 215× for the purpose of identifying cells. Data was obtained and analysed utilising OPUS 7 (Bruker) Software. Spectra with a strong signal to noise ratio were maintained for analysis, 100 per substrate, and were acquired through the culmination of 256 scans at spectral resolution of $4cm^{-1}$.

Both cell lines were seeded on cadmium fluoride IR substrates, within a 12 well plate, at a seeding density of 5×10^4 cells per well/substrate. Following 24 hours incubation at 37°C, the media used during seeding was removed and cells washed thrice with PBS. To each well a 50µg/ml solution of ITC SiNPs was added and the plate incubated for 6 hours. Following the removal of the growth media, cells were washed with PBS on three occasions and 0.9% NaCl, before being fixed with 4% PFA in PBS for 30 minutes. Following this fixing period the resultant cell plates were washed with distilled water, dried at room temperature and refrigerated prior to analysis.

FTIR images were obtained again using the Bruker IFS66V and Hyperion 3000 pieces of equipment, with a standard globar acting as the thermal light source and a 128×128 focal plane array detector (Bruker). Measurements were undertaken with both instruments under a nitrogen atmosphere to reduce variations in the local atmosphere. The measurement conditions for the capture of spectral images were set at 128 scans and a resolution of 8 cm^{-1}. The final images were compiled from a selection of spectral areas characteristic to protein constituents, taking their integrated intensities and adding colour according to their distribution.

3.10 Statistical analysis

Statistical methods throughout this study are represented as mean ± SEM taken over a minimum of three independent experiments. Statistical significance was measured by two-way-ANOVA followed by a Bonferroni post-test using GraphPad

Prism version 5.03 for Windows, GraphPad Software, San Diego California USA.

4. Conclusions

Isothiocyanate-functionalized silicon nanoparticles, their synthesis and the measurement of their optical, chemical and biomedical properties and behaviour were described in this report.

From the MTT assay it was concluded that above concentrations of 15 μg/ml, ITC SiNPs inflicted drastic cytotoxicity on Caco-2 and CCD-841 cells after 48 hours. This outcome is one of mixed interpretations given that clearly cytotoxicity in Caco-2 cells is favourable in the detoxification and/or inhibition of apoptosis in carcinogenic cells, however this highlights that specificity towards cancerous cells is an area in which this research can be developed.

Through confocal microscopy and high resolution synchrotron FTIR, a better understanding as to how and where ITC SiNPs distribute upon cellular internalization was gained. The infrared images and synchrotron IR spectra obtained provided strong evidence for the specific concentration of ITC SiNPs within the nucleus of Caco-2 cells.

Analysis of confocal images and flow cytometry cellular uptake data, it was clear that internalisation of ITC SiNPs within Caco-2 cells was highly time and temperature dependent. From 12 to 48 hours the cellular uptake increased steadily at variable concentration and it was evident that at low temperatures (4 °C) that uptake was hindered in a period monitored up to 24 hours.

The outcomes of this project provide succinct evidence for the versatility of ITC SiNPs as a naturally photoluminescent, easily monitored nano-system for the delivery of anti-cancerous materials. A lot of encouragement can be taken from the results outlined above, a solid base from which future work on these materials can be drawn.

Conflicts of interest

There are no conflicts to declare.

Acknowledgements

X-ray photoelectron spectra were obtained at the National EPSRC XPS Users' Service (NEXUS) at Newcastle University, an EPSRC Mid-Range Facility.

References

1. R. L. Siegel, K. D. Miller and A. Jemal, *CA Cancer J Clin*, 2018, **68**, 7-30.
2. J. Maddams, M. Utley and H. Moller, *Br J Cancer*, 2012, **107**, 1195-1202.
3. A. S. Ahmad, N. Ormiston-Smith and P. D. Sasieni, *Br J Cancer*, 2015, **112**, 943-947.
4. T. S. L. Vincent T. DeVita, Steven A. Rosenberg, Ronald A. DePinho, Robert A. Weinberg.
5. F. P. Downie, H. G. Mar Fan, N. Houede-Tchen, Q. Yi and I. F. Tannock, *Psychooncology*, 2006, **15**, 921-930.
6. X. Wu, Q. H. Zhou and K. Xu, *Acta Pharmacol Sin*, 2009, **30**, 501-512.
7. Y. S. Keum, W. S. Jeong and A. N. Kong, *Mutat Res*, 2004, **555**, 191-202.
8. C. M. M. REX M. , *J. Agric. Food Chem.* , 2004, **52**, 1867-1871.
9. Y. Z. JED W. FAHEY, PAUL TALALAY, *Proc. Natl. Acad. Sci. USA*, 1997, **94**, 10367-10372.
10. J. W. F. Paul T., W. David H., Tory P., Yuesheng Zhang, *Toxicology Letters* 1995, **82/83**, 173-179.
11. R. Munday and C. M. Munday, *Nutr Cancer*, 2002, **44**, 52-59.
12. Haldar, *International Journal of Oncology*, 1992, **33**.
13. A. Pawlik, M. Wala, A. Hac, A. Felczykowska and A. Herman-Antosiewicz, *Phytomedicine*, 2017, **29**, 1-10.
14. Y. Z. JED W. F., PAUL T., *Proc. Natl. Acad. Sci. USA*, 1997, **94**, 10367-10372.
15. E. J. H. Loling Song, Ted Young, Hans J. Tanke *Biophysical Journal*, 1995, **68**, 2588-2600.
16. Y. Zhao, Y. Ye, X. Zhou, J. Chen, Y. Jin, A. Hanson, J. X. Zhao and M. Wu, *Theranostics*, 2014, **4**, 445-459.
17. M. G. B. D. J. Norris, *The American Physical Society*, 1996, **53**, 16338-16346.
18. X. Gao, Y. Cui, R. M. Levenson, L. W. Chung and S. Nie, *Nat Biotechnol*, 2004, **22**, 969-976.
19. N. Lewinski, V. Colvin and R. Drezek, *Small*, 2008, **4**, 26-49.
20. A. M. Derfus, W. C. W. Chan and S. N. Bhatia, *Nano Lett*, 2004, **4**, 11-18.
21. J. Wang, D.-X. Ye, G.-H. Liang, J. Chang, J.-L. Kong and J.-Y. Chen, *J. Mater. Chem. B*, 2014, **2**, 4338-4345.
22. M. D. Lars H. L., Eimer M. T., Andrew H., Benjamin R. H., *Journal of Electroanalytical Chemistry*, 2002, **538-539**, 183-190.
23. M. A. F. B. Shokri, S. I. Hosseini, *Proc. 19th Int. Symp. plasma Chem. Soc.* , 2009.
24. J. N. M. Alun T. Rhys Williams and Stephen A. Winfield, *Analyst*, 1983, **108**, 1067-1071.
25. M. Behray, C. A. Webster, S. Pereira, P. Ghosh, S. Krishnamurthy, W. T. Al-Jamal and Y. Chao, *ACS Appl Mater Interfaces*, 2016, **8**, 8908-8917.
26. J. Wang, S. Sun, F. Peng, L. Cao and L. Sun, *Chem Commun (Camb)*, 2011, **47**, 4941-4943.
27. Y. Zhong, F. Peng, F. Bao, S. Wang, X. Ji, L. Yang, Y. Su, S. T. Lee and Y. He, *J Am Chem Soc*, 2013, **135**, 8350-8356.
28. P. Caravan, J. J. Ellison, T. J. McMurry and R. B. Lauffer, *Chemical Reviews*, 1999, **99**, 2293-2352.
29. S. Jongmin, A. R. Md, K. M. Kyeong, I. G. Ho, L. J. Hee and L. I. Su, *Angewandte Chemie International Edition*, 2009, **48**, 321-324.
30. A. M. Smith, H. Duan, A. M. Mohs and S. Nie, *Advanced drug delivery reviews*, 2008, **60**, 1226-1240.
31. D. He, D. Wang, X. Shi, W. Quan, R. Xiong, C.-y. Yu and H. Huang, *RSC Advances*, 2017, **7**, 12374-12381.
32. L. J. Kan-Zhi Liu, S. M. Kelsey, et al., *Apoptosis*, 2001, **6**, 269-278.
33. J. H. Ahire, Q. Wang, P. R. Coxon, G. Malhotra, R. Brydson, R. Chen and Y. Chao, *ACS Appl Mater Interfaces*, 2012, **4**, 3285-3292.

View Article Online
DOI: 10.1039/C9FD00087A

View Article Online
DOI: 10.1039/C9FD00087A

34. X. Jia, N. Li, W. Zhang, X. Zhang, K. Lapsley, G. Huang, J. Blumberg, G. Ma and J. Chen, *Nutr Cancer*, 2006, **54**, 179-183.
35. C. Xu, X. Yuan, Z. Pan, G. Shen, J. H. Kim, S. Yu, T. O. Khor, W. Li, J. Ma and A. N. Kong, *Mol Cancer Ther*, 2006, **5**, 1918-1926.
36. N. H. Alsharif, C. E. Berger, S. S. Varanasi, Y. Chao, B. R. Horrocks and H. K. Datta, *Small*, 2009, **5**, 221-228.